

Pairing influence in binary nuclear systems

Radu Alexandru GHERGHESCU, Dorin POENARU and Walter GREINER

Radu.Gherghescu@nipne.ro

IFIN-HH, Bucharest-Magurele, Romania

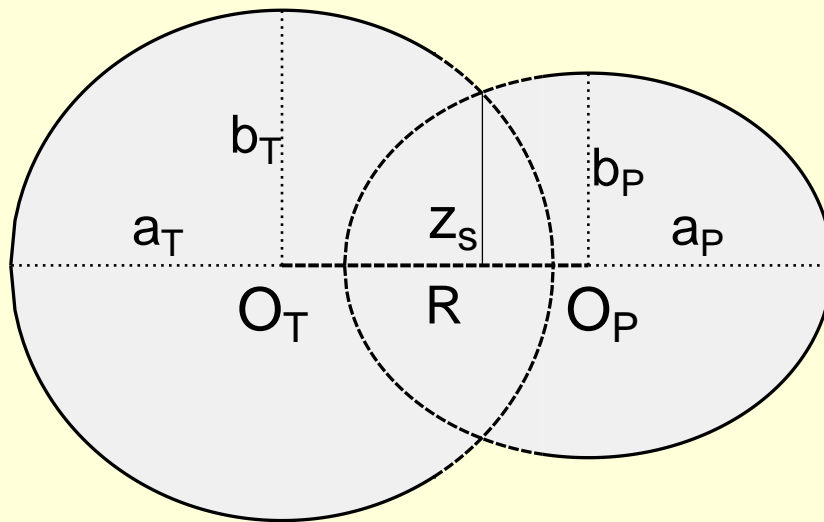
and

Frankfurt Institute for Advanced Studies, J W Goethe University

Frankfurt am Main, Germany

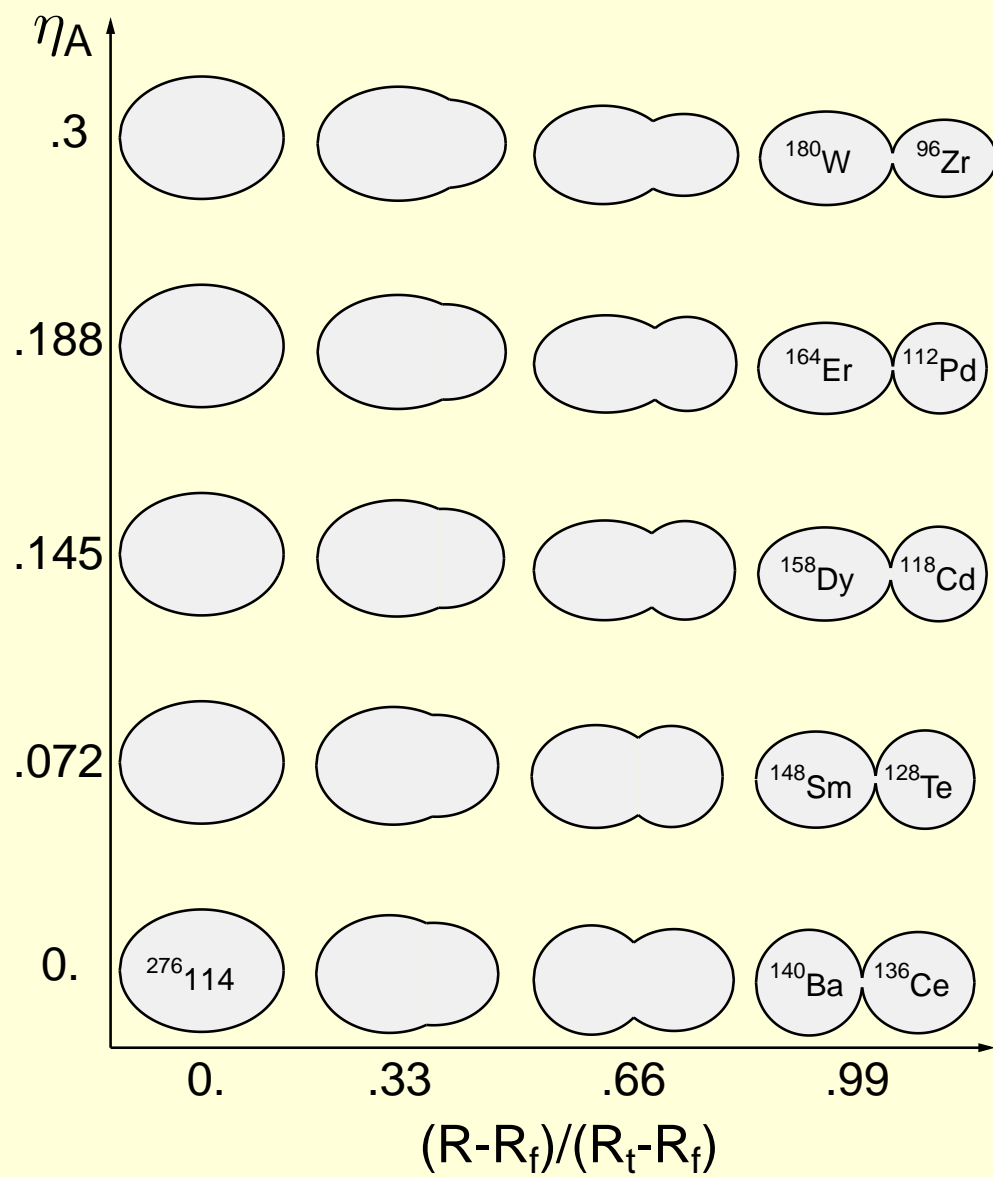
*Symposium on Highlights in Heavy-Ion Physics dedicated to the memory of
Nikola Cindro.*

- Deformation space
- Deformed two-center shell model
- Binary macroscopic-microscopic approach
- Pairing corrections
- Mass tensor and dynamics
- Nuclear inertia
- PES, barriers and penetrabilities for synthesis of $Z=118$ isotopes



1. Mass asymmetry: $\eta = (A_T - A_P)/(A_T + A_P)$
2. Distance between centers: R
3. Deformation parameter of the synthesized (parent) nucleus: b_0/a_0
4. Deformation parameter of the heavy fragment (Target): b_T/a_T
5. Deformation parameter of the light fragment (Projectile): b_P/a_P

Deformation space



Deformed two-center oscillator potential

$$V_{DTCSM}(\rho, z) = \begin{cases} V_1(\rho, z) & , v_1 \\ V_{g1}(\rho, z) & , v_{g1} \\ V_{g2}(\rho, z) & , v_{g2} \\ V_2(\rho, z) & , v_2 \end{cases}$$

where:

$$V_1(\rho, z) = \frac{1}{2}m_o\omega_{\rho_1}^2\rho^2 + \frac{1}{2}m_o\omega_{z_1}^2(z + z_1)^2$$

$$V_{g1}(\rho, z) = 2V_0 - \left[\frac{1}{2}m_o\omega_g^2(\rho - \rho_3)^2 + \frac{1}{2}m_o\omega_g^2(z - z_3)^2 \right]$$

$$V_{g2}(\rho, z) = V_0$$

$$V_2(\rho, z) = \frac{1}{2}m_o\omega_{\rho_2}^2\rho^2 + \frac{1}{2}m_o\omega_{z_2}^2(z - z_2)^2$$

Total Hamiltonian

$$H_{DTCSM} = -\frac{\hbar^2}{2m_0}\Delta + V_{DTCSM}(\rho, z) + V_{\Omega_s} + V_{\Omega^2}$$

separable if $\omega_{\rho_1} = \omega_{\rho_2} = \omega_1$ for a potential:

$$V^{(d)}(\rho, z) = \begin{cases} V_1^{(d)}(\rho, z) = \frac{1}{2}m_0\omega_1^2\rho^2 + \frac{1}{2}m_0\omega_1^2(z + z_1)^2 & , z \leq 0 \\ V_2^{(d)}(\rho, z) = \frac{1}{2}m_0\omega_1^2\rho^2 + \frac{1}{2}m_0\omega_2^2(z - z_2)^2 & , z \geq 0 \end{cases}$$

Diagonalization basis:

$$\Phi_m(\phi) = \frac{1}{\sqrt{2\pi}} \exp(im\phi)$$

$$R_{n_\rho}^{|m|}(\rho) = \left(\frac{2\Gamma(n_\rho+1)\alpha_1^2}{\Gamma(n_\rho+|m|+1)} \right)^{\frac{1}{2}} \exp\left(-\frac{\alpha_1^2\rho^2}{2}\right) (\alpha_1^2\rho^2)^{\frac{|m|}{2}} L_{n_\rho}^{|m|}(\alpha_1^2\rho^2)$$

$$Z_\nu(z) = \begin{cases} C_{\nu_1} \exp\left[-\frac{\alpha_1^2(z+z_1)^2}{2}\right] \mathcal{H}_{\nu_1}[-\alpha_1(z+z_1)] & , z < 0 \\ C_{\nu_2} \exp\left[-\frac{\alpha_2^2(z-z_2)^2}{2}\right] \mathcal{H}_{\nu_2}[\alpha_2(z-z_2)] & , z \geq 0 \end{cases}$$

Oscillator operators:

$$\Delta V_1(\rho, z) = V_1(\rho, z) - V^{(d)}(\rho, z) \quad , v_1$$

$$\Delta V_2(\rho, z) = V_2(\rho, z) - V^{(d)}(\rho, z) \quad , v_2$$

$$\Delta V_g(\rho, z) = V_g(\rho, z) \quad , v_g$$

Spin-orbit l_s and l^2 potentials:

$$V_{l_s} = \begin{cases} - \left\{ \frac{\hbar}{m_0 \omega_{01}} \kappa_1(\rho, z), (\nabla V \times \mathbf{p})_s \right\} & , A_1 - region \\ - \left\{ \frac{\hbar}{m_0 \omega_{02}} \kappa_2(\rho, z), (\nabla V \times \mathbf{p})_s \right\} & , A_2 - region \end{cases}$$

$$V_{l^2} = \begin{cases} - \left\{ \frac{\hbar}{m_0^2 \omega_{01}^3} \kappa_1 \mu_1(\rho, z), (\nabla V \times \mathbf{p})^2 \right\} & , A_1 - region \\ - \left\{ \frac{\hbar}{m_0^2 \omega_{02}^3} \kappa_2 \mu_2(\rho, z), (\nabla V \times \mathbf{p})^2 \right\} & , A_2 - region \end{cases}$$

Spin-orbit l_s and l^2 operators

General expression:

$$l_s \rightarrow \frac{1}{2}(\Omega^+ s^- + \Omega^- s^+) + \Omega_z s_z$$

Shape dependent Ω - operators:

$$\begin{aligned}\Omega^+(v_1) &= -e^{i\varphi} \left[\frac{\partial V_1(\rho, z)}{\partial \rho} \frac{\partial}{\partial z} - \frac{\partial V_1(\rho, z)}{\partial z} \frac{\partial}{\partial \rho} - \frac{i}{\rho} \frac{\partial V_1(\rho, z)}{\partial z} \frac{\partial}{\partial \varphi} \right] \\ &= -e^{i\varphi} \left[m_0 \omega_{\rho_1}^2 \rho \frac{\partial}{\partial z} - m_0 \omega_{z_1}^2 (z + z_1) \frac{\partial}{\partial \rho} - \frac{i}{\rho} m_0 \omega_{z_1}^2 (z + z_1) \frac{\partial}{\partial \varphi} \right]\end{aligned}$$

$$\begin{aligned}\Omega^-(v_1) &= e^{-i\varphi} \left[\frac{\partial V_1(\rho, z)}{\partial \rho} \frac{\partial}{\partial z} - \frac{\partial V_1(\rho, z)}{\partial z} \frac{\partial}{\partial \rho} + \frac{i}{\rho} \frac{\partial V_1(\rho, z)}{\partial z} \frac{\partial}{\partial \varphi} \right] \\ &= e^{-i\varphi} \left[m_0 \omega_{\rho_1}^2 \rho \frac{\partial}{\partial z} - m_0 \omega_{z_1}^2 (z + z_1) \frac{\partial}{\partial \rho} + \frac{i}{\rho} m_0 \omega_{z_1}^2 (z + z_1) \frac{\partial}{\partial \varphi} \right]\end{aligned}$$

$$\begin{aligned}\Omega_z(v_1) &= -\frac{i}{\rho} \frac{\partial V_1}{\partial \rho} \frac{\partial}{\partial \varphi} \\ &= -i m_0 \omega_{\rho_1}^2 \frac{\partial}{\partial \varphi}\end{aligned}$$

Total spin-orbit operators:

$$V_{\Omega s}(v_1) = -\frac{\hbar}{m_0\omega_{01}}\kappa_1\{\Omega s(v_1), (v_1)\}$$

$$V_{\Omega s}(v_2) = -\frac{\hbar}{m_0\omega_{02}}\kappa_2\{\Omega s(v_2), (v_2)\}$$

$$V_{\Omega s}(v_g) = -\frac{\hbar}{m_0\omega_{01}}\kappa_1\{\Omega s(v_{g1}), (v_{g1})\} - \frac{\hbar}{m_0\omega_{02}}\kappa_2\{\Omega s(v_{g2}), (v_{g2})\}$$

Total matrix elements:

$$\begin{aligned} \langle i | \text{DTCSM} | j \rangle = & E_{osc}^{(d)}(n_\rho, |m|, \nu) + \langle i | \Delta V_1 | j \rangle + \langle i | \Delta V_2 | j \rangle \\ & + \langle i | V_g | j \rangle + \langle i | V_{\Omega s} | j \rangle + \langle i | V_{\Omega^2} | j \rangle \end{aligned}$$

where $E_{osc}^{(d)}$ is the diagonalized oscillator energy:

$$E_{osc}^{(d)} = \hbar\omega_1(2n_\rho + |m| + 1) + \hbar\omega_1(\nu_1 + 0.5)$$

Diagonalization: one obtains the total binary s.p.s. energy levels $\{\epsilon_k\}$, as input data for the calculation of **shell** and **pairing** corrections.

$\{E_{sp}\} \rightarrow \epsilon_i$: input data to calculate E_{shell} :

$$\delta u = \sum_i \epsilon_i - \tilde{U}$$

Smoothing $\Rightarrow \tilde{U}$:

(1) smoothed level distribution $\tilde{g}(\epsilon)$:

$$\begin{aligned} \tilde{g}(\epsilon) &= \frac{1}{\gamma} \int_{-\infty}^{\infty} \zeta\left(\frac{\epsilon - \epsilon'}{\gamma}\right) g(\epsilon') d\epsilon' \\ &= \frac{1}{\gamma} \sum_{i=1}^{\infty} \zeta\left(\frac{\epsilon - \epsilon_i}{\gamma}\right) \end{aligned}$$

where the smoothing function:

$$\zeta(x) = \frac{1}{\sqrt{\pi}} \exp(-x^2) \sum_{k=0}^m a_{2k} H_{2k}(x)$$

(2) Then the smoothed part \rightarrow smearing :

$$\tilde{U} = \hbar\omega = \int_{\infty}^{\tilde{\lambda}} \tilde{g}(\epsilon) \epsilon d\epsilon$$

(3) where the *smoothed* Fermi level comes from N_e conservation.

Pairing interaction

Normally $Z/2$ levels are occupied, BUT only n levels below and n' levels above the Fermi energy contribute to the pairing interaction.

If Ω is the cutoff energy, $n = n' = \Omega \tilde{g}_s / 2$ and $\tilde{\Delta} = 12 / \sqrt{A} \hbar \omega_0^0$.

BCS equations:

$$0 = \sum_{k_i}^{k_f} \frac{\epsilon_k - \lambda}{\sqrt{(\epsilon_k - \lambda)^2 + \Delta^2}}$$

$$\frac{2}{G} = \sum_{k_i}^{k_f} \frac{1}{\sqrt{(\epsilon_k - \lambda)^2 + \Delta^2}}$$

$$k_i = Z/2 - n + 1, \quad k_f = Z/2 + n',$$

Suppose the pairing strength G is the same for uniform distribution:

$$\frac{2}{G} \simeq 2\tilde{g}(\tilde{\lambda}) \ln \left(\frac{2\Omega}{\tilde{\Delta}} \right)$$

Pairing interaction

As a consequence of the pairing correlation, the levels below the Fermi energy are only partially filled, while those above the Fermi energy are partially empty.

IF $\{\epsilon_k\}$ are the DTCSM single particle energies, then:

$$v_k^2 = [1 - (\epsilon_k - \lambda)/E_k] / 2$$

and

$$u_k^2 = 1 - v_k^2$$

where the quasi-particle energy is:

$$E_k = \sqrt{(\epsilon_k - \lambda)^2 + \Delta^2}.$$

where λ and Δ are the solutions of the BCS system of equations.

Pairing interaction

The pairing correction:

$$\delta p = p - \tilde{p}$$

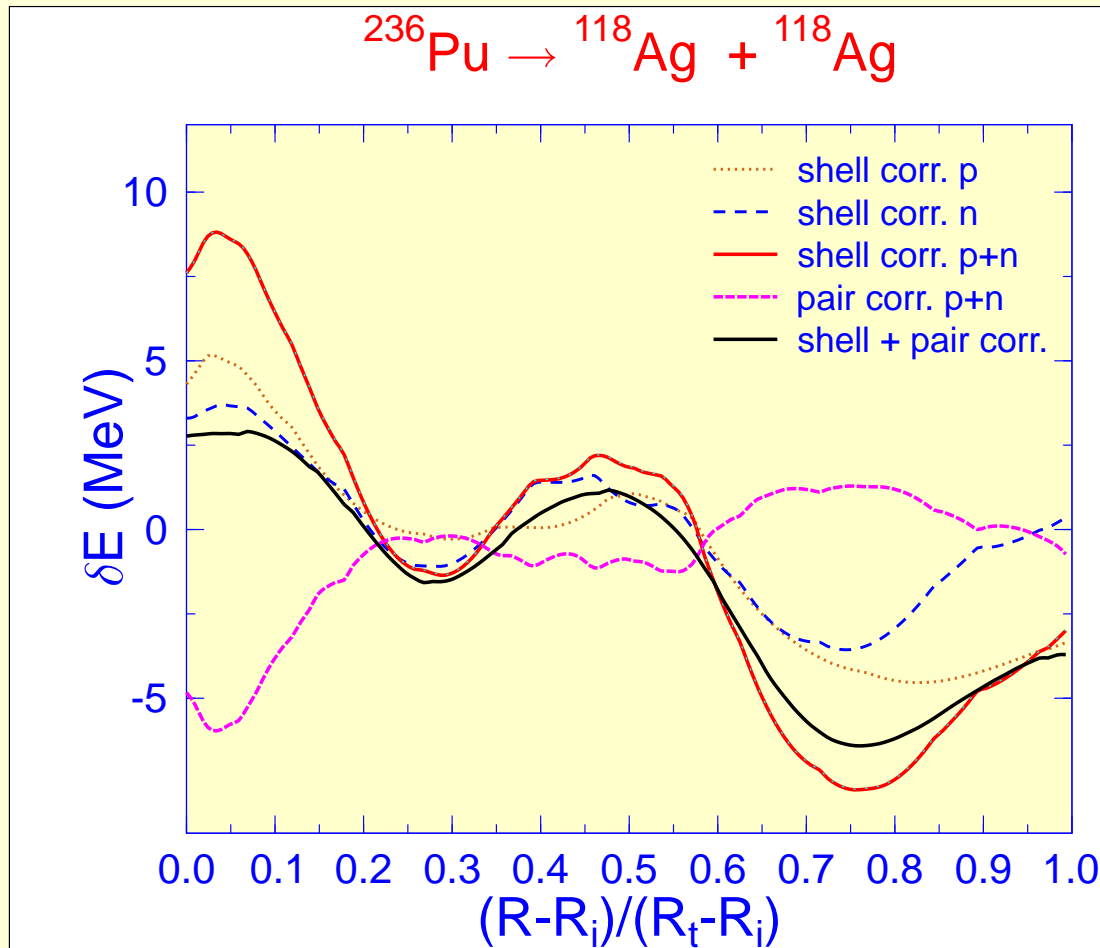
represents the difference between the pairing correlation energies for the discrete level distribution:

$$p = \sum_{k=k_i}^{k_f} 2v_k^2 \epsilon_k - 2 \sum_{k=k_i}^{Z/2} \epsilon_k - \frac{\Delta^2}{G}$$

and for the continuous level distribution

$$\tilde{p} = -(\tilde{g}\tilde{\Delta}^2)/2 = -(\tilde{g}_s\tilde{\Delta}^2)/4$$

Compared to shell correction, the pairing correction is out of phase and smaller. One has again $\delta p = \delta p_p + \delta p_n$, and $\delta e = \delta u + \delta p$.



Shell and pairing corrections for ^{236}Pu . The s.p.s. were obtained with the two-center shell model.

Macroscopic energy

The macroscopic energy: the sum of Coulomb E_C and Yukawa E_Y :

$$E_C = \frac{2\pi}{3} \rho_e \int_{z_{min}}^{z_{max}} dz \int_{z_{min}}^{z_{max}} dz' \cdot F_C(z, z')$$

where $F_C(z, z')$ - shape dependent \rightarrow binary fusion configuration:

$$E_C = \frac{2\pi}{3} (\rho_{e1}^2 F_{C1} + \rho_{e2}^2 F_{C2} + 2\rho_{e1}\rho_{e2} F_{C12})$$

where ρ_{e1} and ρ_{e2} are the charge densities, and:

$$E_Y = \frac{1}{4\pi r_0^2} [c_{s1} F_{EY1} + c_{s2} F_{EY2} + 2(c_{s1}c_{s2})^{1/2} F_{EY12}]$$

The total deformation energy: $E_{def} = E_C + E_Y + \delta u + \delta p$ The surface energy constants:

$$c_{si} = a_s (1 - \kappa I_i^2) \quad \text{where}$$

$$I_i = (N_{ix} - Z_{ix}) / A_{ix}$$

Deformation variable evolution

Variation of the semiaxis ratios: $\chi_T = b_T/a_T$ and $\chi_P = b_P/a_P$:

$$\chi_T = \chi_{T0} + (\chi_0 - \chi_{T0}) \exp \left[- \left(\frac{R - R_{k_T}}{R_t - R_f} k_T \right)^2 \right]$$
$$\chi_P = \chi_{P0} + (\chi_{Pf} - \chi_{P0}) \exp \left[- \left(\frac{R - R_{k_P}}{R_t - R_f} k_P \right)^2 \right]$$

where:

$$\chi_{Pf} = \chi_{P0} - \frac{i_P}{10} (\chi_0 - \chi_{P0})$$

Free variables \rightarrow functions of R :

$$b_P = b_P(k_T, k_P, i_P; R)$$

$$\chi_T = \chi_T(k_T, k_P, i_P; R)$$

$$\chi_P = \chi_P(k_T, k_P, i_P; R)$$

Mass tensor and dynamics

Cranking model \rightarrow Tensor contraction along R :

$$\begin{aligned} B(R) = & B_{b_P b_P} \left(\frac{db_P}{dR} \right)^2 + 2B_{b_P \chi_T} \frac{db_P}{dR} \frac{d\chi_T}{dR} + 2B_{b_P \chi_P} \frac{db_P}{dR} \frac{d\chi_P}{dR} + \\ & 2B_{b_P R} \frac{db_P}{dR} + B_{\chi_T \chi_T} \left(\frac{d\chi_T}{dR} \right)^2 + 2B_{\chi_T \chi_P} \frac{d\chi_T}{dR} \frac{d\chi_P}{dR} + \\ & 2B_{\chi_T R} \frac{d\chi_T}{dR} + B_{\chi_P \chi_P} \left(\frac{d\chi_P}{dR} \right)^2 + 2B_{\chi_P R} \frac{d\chi_P}{dR} + B_{RR} \end{aligned}$$

Penetrability P for a given fusion path (*fus*):

$$P = \exp(-K_{ov})$$

where

$$K_{ov}(b_P, \kappa_T, \kappa_P; R) = \frac{2}{\hbar} \int_{(fus)} [2B(R)_{b_P, \kappa_T, \kappa_P} E_{def}(R)_{b_P, \kappa_T, \kappa_P}]^{1/2} dR$$

Cranking mass tensor

Cranking model → Tensor contraction along R results in scalar forms:

$$B_\varepsilon = 2\hbar^2 \sum_{\nu\mu} \frac{\langle \nu | \partial V_{DTCSM} / \partial \varepsilon | \mu \rangle \langle \mu | \partial V_{DTCSM} / \partial \varepsilon | \nu \rangle}{(E_\nu + E_\mu)^3} (u_\nu v_\mu + u_\mu v_\nu)^2$$

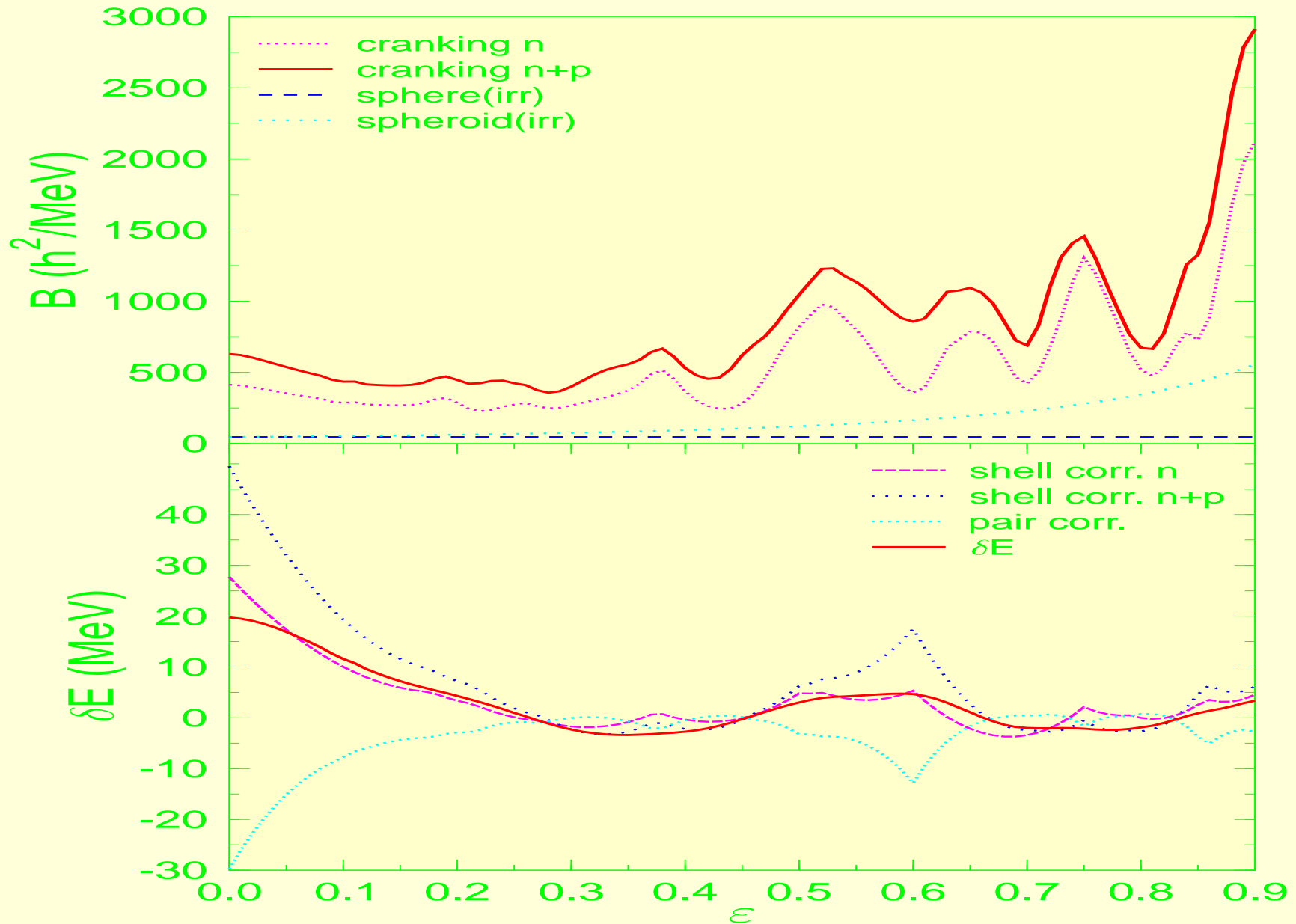
where:

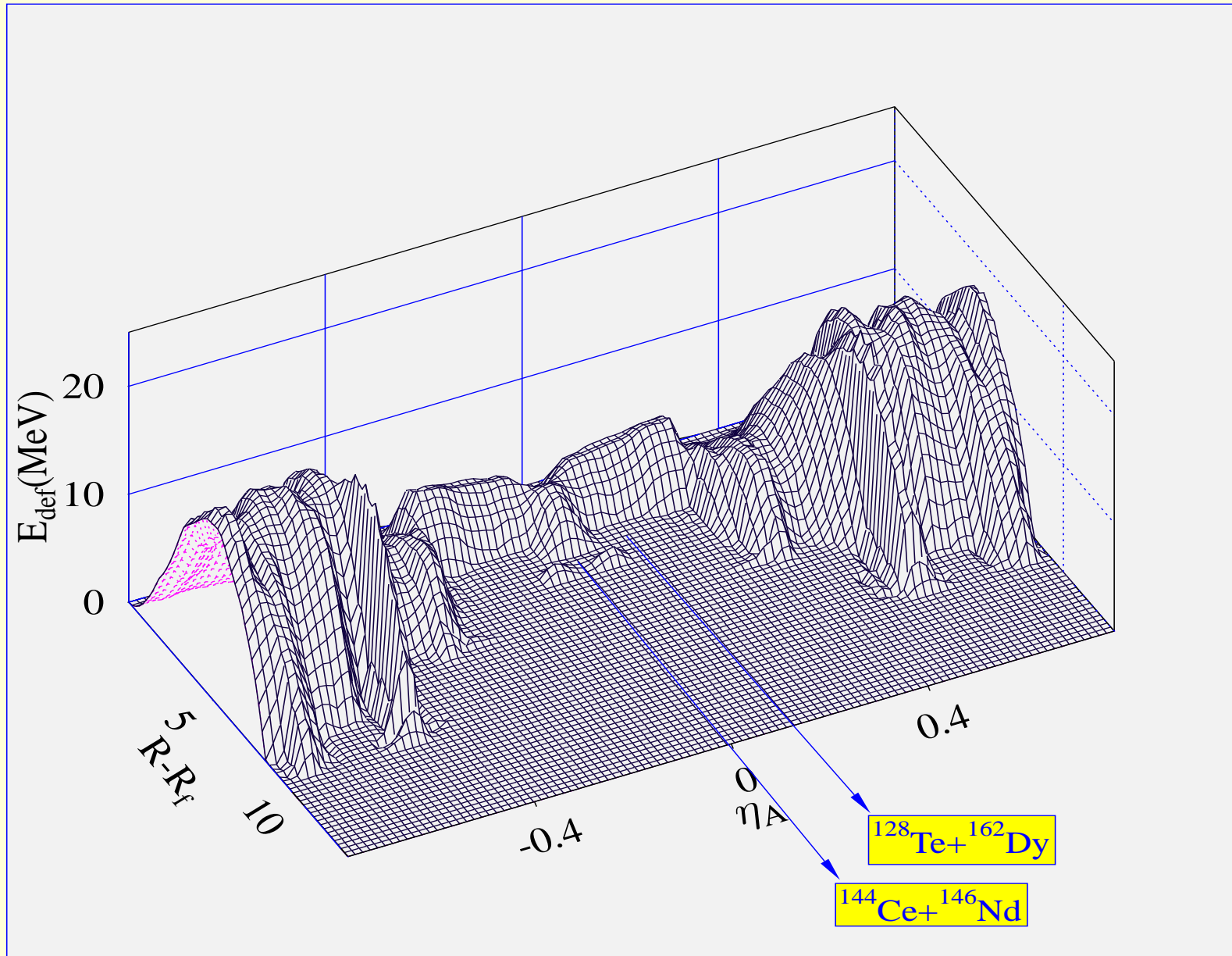
$$V_{DTCSM} = V_{DTCSM}^{2osc} + V_{l_s} + V_{l_2}$$

and the s. p. s. are the DTCSM wave functions.

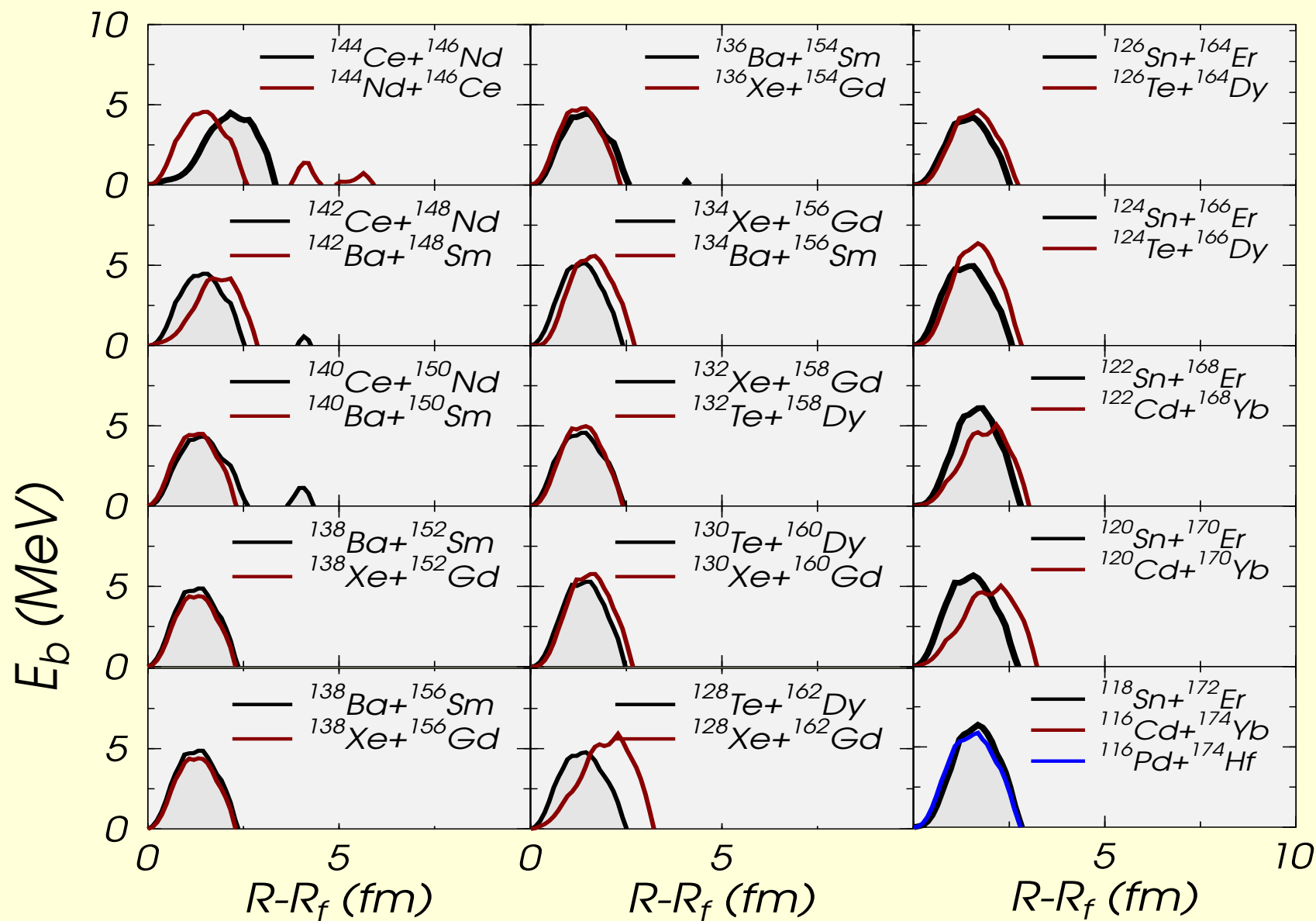
$$|\mu\rangle = |DTCSM(n_\rho, n_z, m | \rho, z, \phi)\rangle$$

Cranking inertia for ^{236}Pu



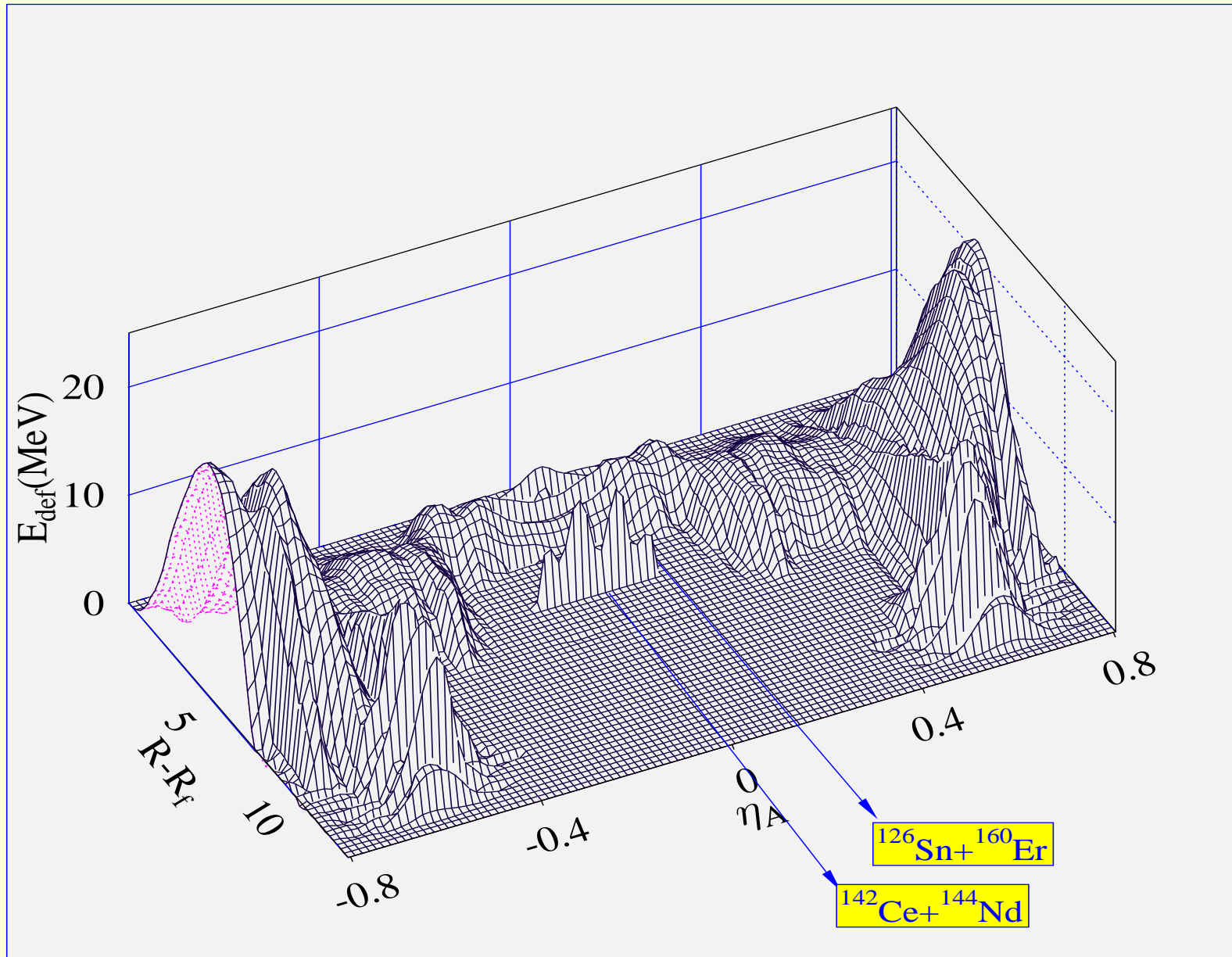


Isobaric channel cold fusion barriers for $^{290}_{118}$

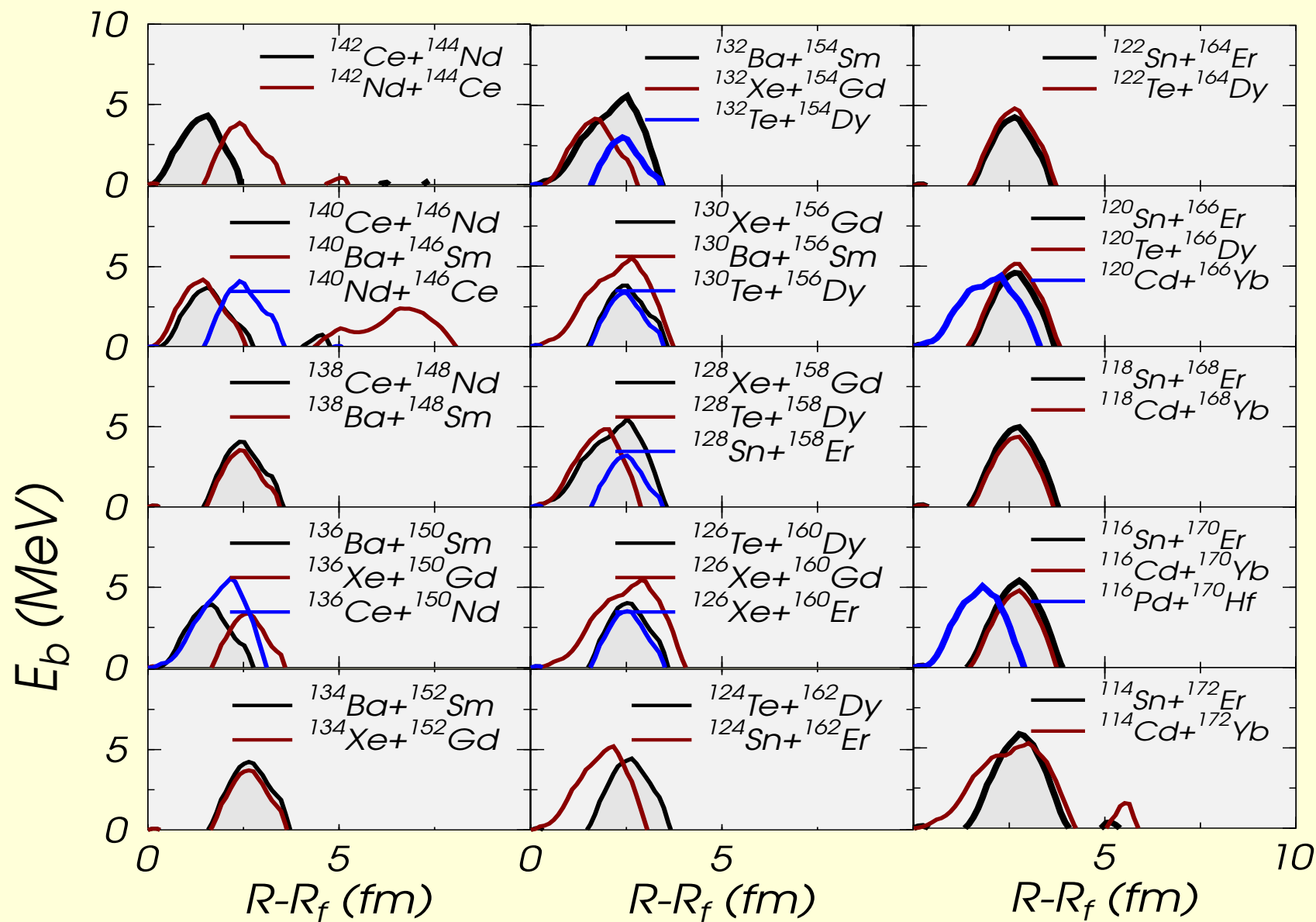


Cold fusion channels for $^{290}\text{118}$

Reaction	E_b (MeV)	$\log_{10}P$	Reaction	E_b (MeV)	$\log_{10}P$
$^{144}\text{Ce}+^{146}\text{Nd}$	4.4	-5.	$^{132}\text{Xe}+^{158}\text{Gd}$	4.57	-4.31
$^{144}\text{Nd}+^{146}\text{Ce}$	4.56	-5.89	$^{132}\text{Te}+^{158}\text{Dy}$	4.98	-4.49
$^{142}\text{Ce}+^{148}\text{Nd}$	4.47	-4.51	$^{130}\text{Xe}+^{160}\text{Gd}$	5.77	-5.19
$^{142}\text{Ba}+^{148}\text{Sm}$	4.2	-4.52	$^{130}\text{Te}+^{160}\text{Dy}$	5.29	-4.76
$^{140}\text{Ce}+^{150}\text{Nd}$	4.35	-4.91	$^{128}\text{Te}+^{162}\text{Dy}$	4.77	-4.44
$^{140}\text{Ba}+^{150}\text{Sm}$	4.5	-4.17	$^{128}\text{Xe}+^{162}\text{Gd}$	5.91	-6.27
$^{138}\text{Ba}+^{152}\text{Sm}$	4.86	-4.42	$^{128}\text{Sn}+^{162}\text{Er}$	5.19	-4.6
$^{138}\text{Xe}+^{152}\text{Gd}$	4.4	-4.04	$^{126}\text{Te}+^{164}\text{Dy}$	5.87	-5.32
$^{136}\text{Ba}+^{154}\text{Sm}$	4.44	-4.33	$^{126}\text{Sn}+^{164}\text{Er}$	5.48	-4.81
$^{136}\text{Xe}+^{154}\text{Gd}$	4.66	-4.33	$^{124}\text{Sn}+^{166}\text{Er}$	4.96	-4.64
$^{134}\text{Ba}+^{156}\text{Sm}$	5.58	-5.02	$^{124}\text{Te}+^{166}\text{Dy}$	6.37	-5.68
$^{134}\text{Xe}+^{156}\text{Gd}$	5.13	-4.61	$^{122}\text{Sn}+^{168}\text{Er}$	6.12	-5.5
$^{132}\text{Xe}+^{158}\text{Gd}$	4.57	-4.31	$^{122}\text{Cd}+^{168}\text{Yb}$	5.07	-5.39



Isobaric channel cold fusion barriers for $^{286}118$

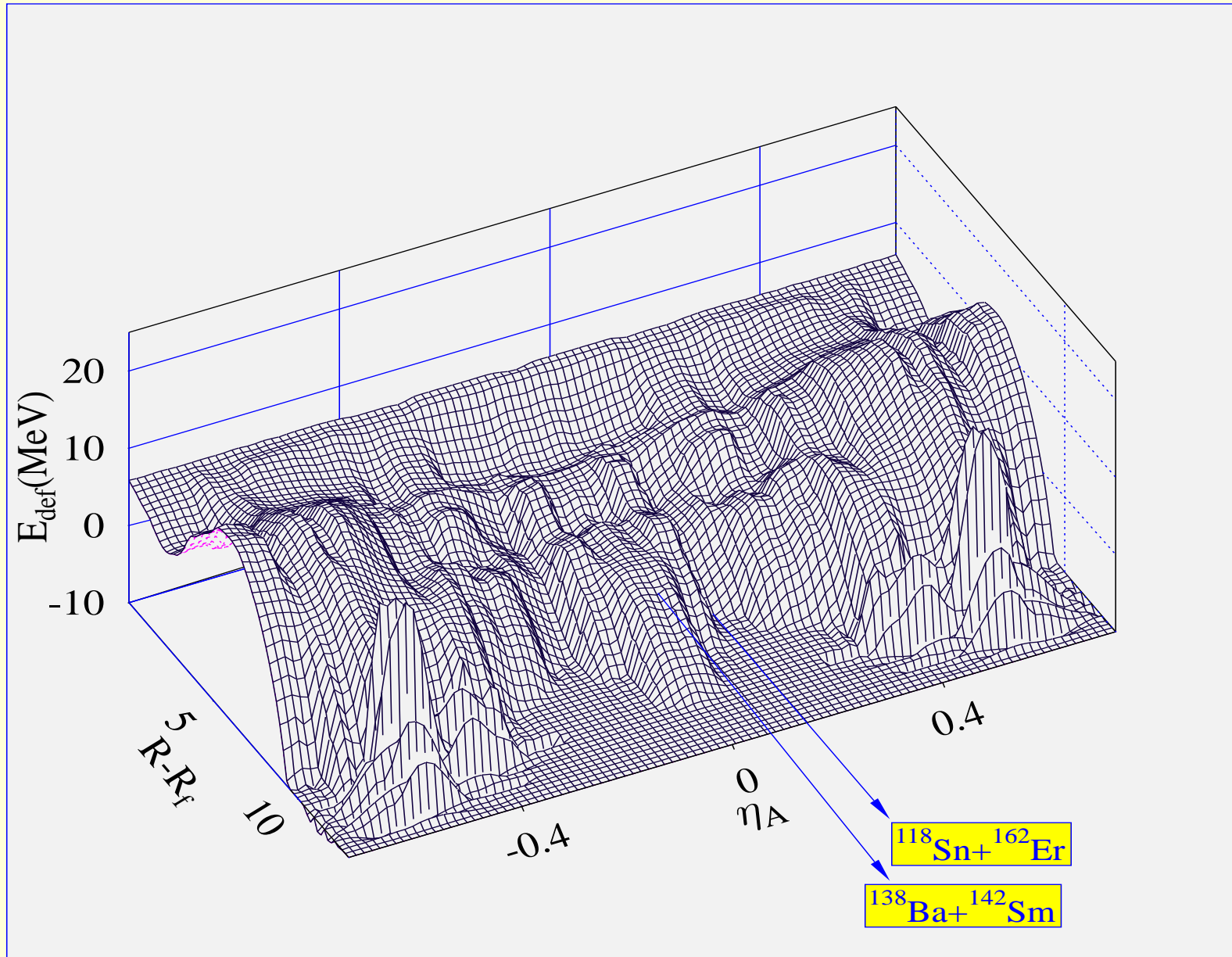


Cold fusion channels for $^{286}\text{118}$

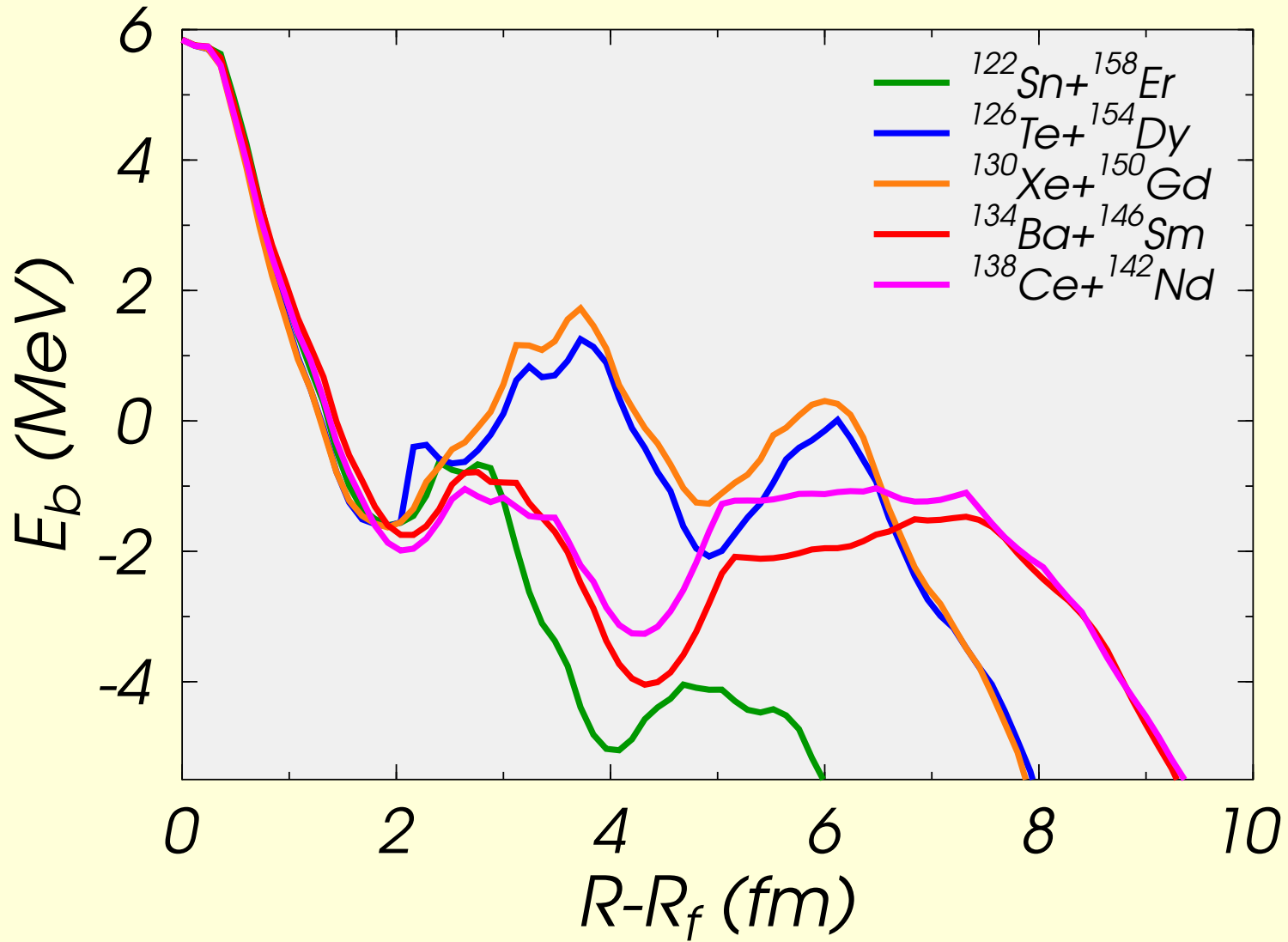
Reaction	E_b (MeV)	$\log_{10}P$	Reaction	E_b (MeV)	$\log_{10}P$
$^{142}\text{Ce}+^{144}\text{Nd}$	4.3	-3.48	$^{132}\text{Ba}+^{154}\text{Sm}$	5.6	-5.55
$^{142}\text{Nd}+^{144}\text{Ce}$	3.85	-3.53	$^{132}\text{Xe}+^{154}\text{Gd}$	4.18	-3.63
$^{140}\text{Ce}+^{146}\text{Nd}$	3.7	-3.7	$^{132}\text{Te}+^{154}\text{Dy}$	3.02	-2.4
$^{140}\text{Nd}+^{146}\text{Ce}$	4.1	-3.4	$^{130}\text{Ba}+^{156}\text{Sm}$	5.52	-6.25
$^{140}\text{Ba}+^{146}\text{Sm}$	4.19	-8.71	$^{130}\text{Xe}+^{156}\text{Gd}$	3.79	-3.18
$^{138}\text{Ce}+^{148}\text{Nd}$	4.06	-3.35	$^{130}\text{Te}+^{156}\text{Dy}$	3.34	-2.71
$^{138}\text{Ba}+^{148}\text{Sm}$	3.54	-2.83	$^{128}\text{Sn}+^{158}\text{Er}$	3.2	-2.56
$^{136}\text{Ba}+^{150}\text{Sm}$	3.92	-3.39	$^{128}\text{Xe}+^{158}\text{Gd}$	5.48	-5.82
$^{136}\text{Ce}+^{150}\text{Nd}$	5.54	-4.86	$^{128}\text{Te}+^{158}\text{Dy}$	4.85	-4.22
$^{136}\text{Xe}+^{150}\text{Gd}$	3.37	-2.69	$^{126}\text{Xe}+^{160}\text{Gd}$	5.44	-6.58
$^{134}\text{Ba}+^{152}\text{Sm}$	4.23	-3.49	$^{126}\text{Te}+^{160}\text{Dy}$	4.02	-3.33
$^{134}\text{Xe}+^{152}\text{Gd}$	3.71	-3.06	$^{126}\text{Sn}+^{160}\text{Er}$	3.51	-2.9

Cold fusion channels for $^{286}\text{118}$

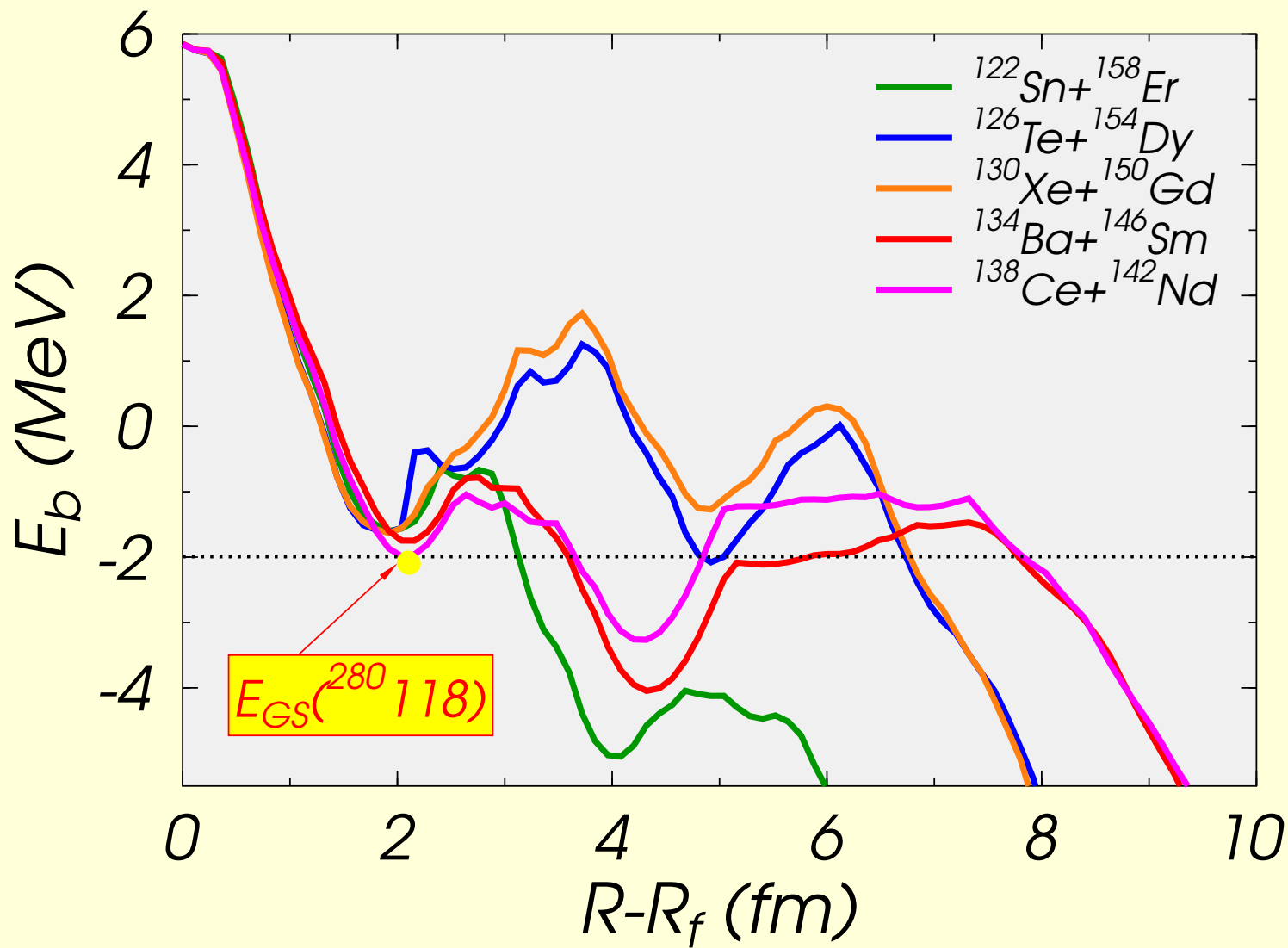
Reaction	E_b (MeV)	$\log_{10}P$	Reaction	E_b (MeV)	$\log_{10}P$
$^{124}\text{Sn}+^{162}\text{Er}$	5.2	-4.55	$^{118}\text{Sn}+^{168}\text{Er}$	4.98	-4.11
$^{124}\text{Te}+^{162}\text{Dy}$	4.44	-3.65	$^{118}\text{Cd}+^{168}\text{Yb}$	4.37	-3.6
$^{122}\text{Te}+^{164}\text{Dy}$	4.82	-3.93	$^{116}\text{Sn}+^{170}\text{Er}$	5.42	-4.5
$^{122}\text{Sn}+^{164}\text{Er}$	4.27	-3.47	$^{116}\text{Cd}+^{170}\text{Yb}$	4.8	-3.93
$^{120}\text{Te}+^{166}\text{Dy}$	5.14	-4.28	$^{116}\text{Pd}+^{170}\text{Hf}$	5.08	-4.6
$^{120}\text{Sn}+^{166}\text{Er}$	4.59	-3.75	$^{114}\text{Sn}+^{172}\text{Er}$	5.87	-5.27



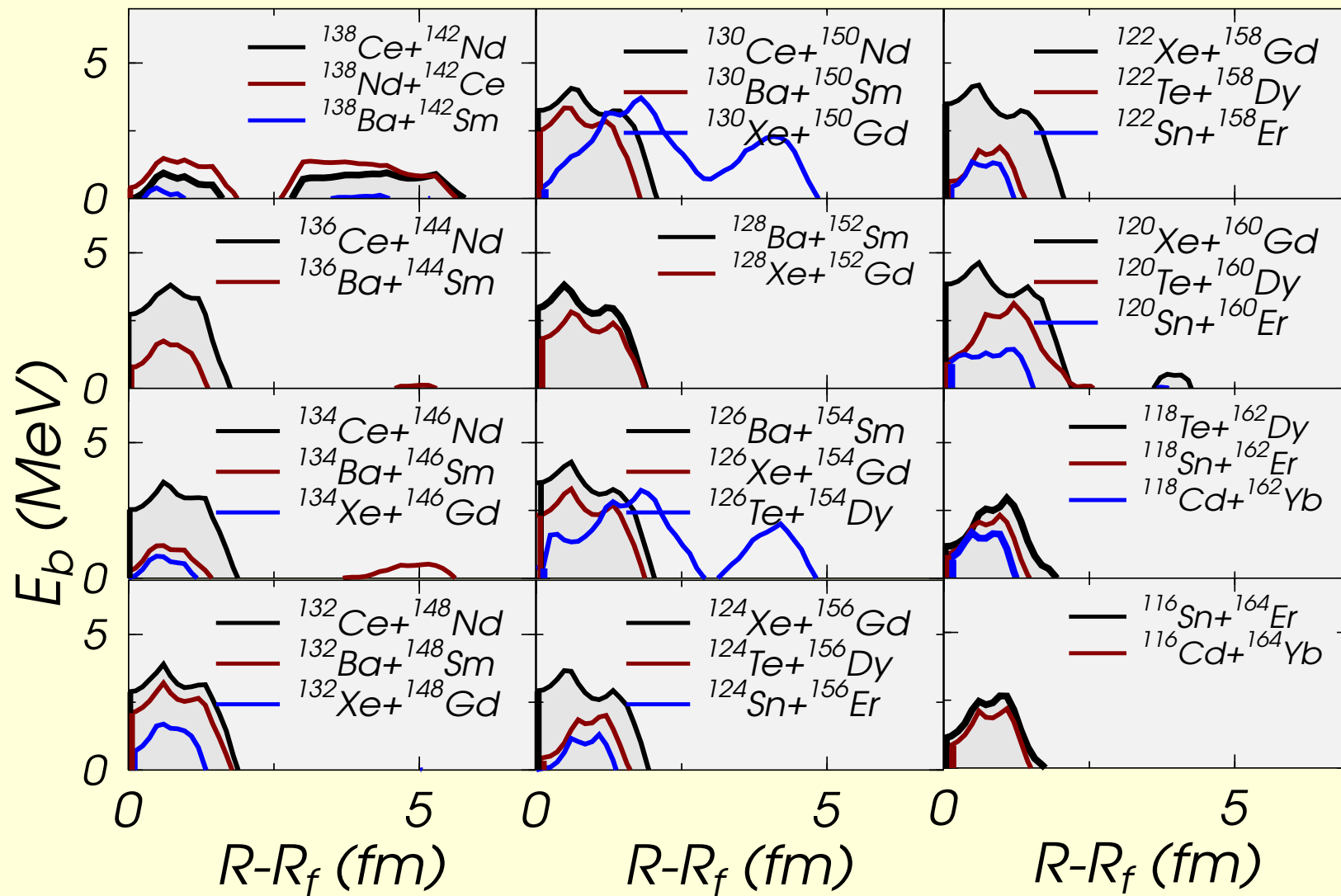
Cold fusion barriers for $^{280}\text{118}$



Cold fusion barriers for $^{280}118$



Isobaric channel cold fusion channels for $^{280}118$



Cold fusion channels for $^{280}\text{118}$

Reaction	E_b (MeV)	$\log_{10}P$	Reaction	E_b (MeV)	$\log_{10}P$
$^{138}\text{Nd}+^{142}\text{Ce}$	1.48	-5.22	$^{130}\text{Ce}+^{150}\text{Nd}$	4.07	-4.32
$^{138}\text{Ce}+^{142}\text{Nd}$	0.95	-3.94	$^{130}\text{Ba}+^{150}\text{Sm}$	3.34	-3.28
$^{138}\text{Ba}+^{142}\text{Sm}$	0.39	-0.59	$^{130}\text{Xe}+^{150}\text{Gd}$	3.71	-7.87
$^{136}\text{Ce}+^{144}\text{Nd}$	3.81	-3.31	$^{128}\text{Ba}+^{152}\text{Sm}$	3.8	-3.7
$^{136}\text{Ba}+^{144}\text{Sm}$	1.61	-1.91	$^{128}\text{Xe}+^{152}\text{Gd}$	2.82	-3.
$^{134}\text{Ce}+^{146}\text{Nd}$	3.54	-3.56	$^{126}\text{Ba}+^{154}\text{Sm}$	4.28	-4.34
$^{134}\text{Ba}+^{146}\text{Sm}$	1.2	-2.4	$^{126}\text{Xe}+^{154}\text{Gd}$	3.29	-3.32
$^{134}\text{Xe}+^{146}\text{Gd}$	0.81	-0.77	$^{126}\text{Te}+^{154}\text{Dy}$	3.24	-6.72
$^{132}\text{Ce}+^{148}\text{Nd}$	3.9	-3.81	$^{124}\text{Xe}+^{156}\text{Gd}$	3.67	-3.79
$^{132}\text{Ba}+^{148}\text{Sm}$	2.88	-3.09	$^{124}\text{Te}+^{156}\text{Dy}$	2.01	-1.9
$^{132}\text{Xe}+^{148}\text{Gd}$	1.69	-1.58	$^{124}\text{Sn}+^{156}\text{Er}$	1.17	-1.15

Cold fusion channels for $^{280}118$

Reaction	E_b (MeV)	$\log_{10}P$	Reaction	E_b (MeV)	$\log_{10}P$
$^{122}\text{Xe}+^{158}\text{Gd}$	4.18	-4.38	$^{118}\text{Te}+^{162}\text{Dy}$	2.95	-2.83
$^{122}\text{Te}+^{158}\text{Dy}$	1.9	-1.75	$^{118}\text{Sn}+^{162}\text{Er}$	2.32	-2.07
$^{122}\text{Sn}+^{158}\text{Er}$	1.32	-1.31	$^{118}\text{Cd}+^{162}\text{Yb}$	1.68	-1.57
$^{120}\text{Xe}+^{160}\text{Gd}$	4.63	-5.37	$^{116}\text{Sn}+^{164}\text{Er}$	2.66	-2.53
$^{120}\text{Te}+^{160}\text{Dy}$	3.13	-3.43	$^{116}\text{Cd}+^{164}\text{Yb}$	1.99	-2.04
$^{120}\text{Sn}+^{160}\text{Er}$	1.31	-1.86			

Possible conclusions

- A specialized binary macroscopic-microscopic model is applied to calculate the deformation energy.
- Cranking mass tensor and multidimensional minimization of action integral is used to obtain WKB penetrabilities.

● For ²⁹⁴118:

$$^{136}\text{Te} + ^{158}\text{Dy} \rightarrow \log P = -5.97$$

$$^{126}\text{Sn} + ^{168}\text{Er} \rightarrow \log P = -6.55$$

For ²⁹⁰118:

$$^{140}\text{Ba} + ^{150}\text{Sm} \rightarrow \log P = -4.17$$

$$^{128}\text{Te} + ^{162}\text{Dy} \rightarrow \log P = -4.44$$

$$^{116}\text{Pd} + ^{174}\text{Hf} \rightarrow \log P = -4.6$$

● For ²⁸⁶118:

$$^{138}\text{Ba} + ^{148}\text{Sm} \rightarrow \log P = -2.83$$

$$^{132}\text{Te} + ^{154}\text{Dy} \rightarrow \log P = -2.4$$

$$^{126}\text{Pd} + ^{160}\text{Hf} \rightarrow \log P = -2.9$$

For ²⁸⁰118:

$$^{138}\text{Ba} + ^{142}\text{Sm} \rightarrow \log P = -0.59$$

$$^{134}\text{Xe} + ^{146}\text{Gd} \rightarrow \log P = -0.77$$

$$^{124}\text{Sn} + ^{156}\text{Er} \rightarrow \log P = -1.15$$

$$^{122}\text{Sn} + ^{158}\text{Er} \rightarrow \log P = -1.31$$